

## THE SPL (II) AT CERN, A SUPERCONDUCTING 3.5 GeV H<sup>-</sup> LINAC

F. Gerigk, G. Bellodi, E. Benedico Mora, Y. Body, F. Caspers, R. Garoby, K. Hanke, C. Hill, J. Inigo-Golfin, K. Kahle, T. Kroyer, D. Kuechler, J.-B. Lallement, M. Lindroos, A.M. Lombardi, A. Lopez Hernandez, M. Magistris, T.K. Meinschad, A. Millich, E. Noah Messomo, M. Paoluzzi, M. Pasini, C. Rossi, J.P. Royer, M. Sanmarti, E. Sargsyan, R. Scrivens, M. Silari, T. Steiner, J. Tückmantel, M. Vretenar, CERN, Geneva, M. Baylac, J.M. De Conto, E. Froidefond, LPSC Grenoble, S. Chel, R. Duperrier, D. Uriot, CEA Saclay, M. Hori, CERN/Tokyo University, C. Pagani, P. Pierini, INFN Milan, V. Palladino, INFN Naples

### Abstract

A revision of the physics needs and recent progress in the technology of superconducting (SC) RF cavities have triggered major changes in the design of a SC H<sup>-</sup> linac at CERN. With up to 5 MW beam power, the SPL can be the proton driver for a next generation ISOL-type radioactive beam facility ("EURISOL") and/or supply protons to a neutrino ( $\nu$ ) facility (conventional superbeam + beta-beam or  $\nu$ -factory). Furthermore the SPL can replace Linac2 and the PS booster (PSB), improving significantly the beam performance in terms of brightness, intensity, and reliability for the benefit of all proton users at CERN, including LHC and its luminosity upgrade. Compared with the first conceptual design, the beam energy is almost doubled (3.5 GeV instead of 2.2 GeV) while the length is reduced by 40%. At a repetition rate of 50 Hz, the linac reuses decommissioned 352.2 MHz RF equipment from LEP in the low-energy part. Beyond 90 MeV the RF frequency is doubled, and from 180 MeV onwards high-gradient SC bulk-niobium cavities accelerate the beam to its final energy of 3.5 GeV. This paper presents the overall design approach, together with the technical progress since the first conceptual design in 2000.

### INTRODUCTION

The first SPL design (SPL I) [1] was driven by the idea to reuse decommissioned LEP RF equipment (klystrons, SC cavities) for the construction of a SC proton driver for a CERN-based  $\nu$ -factory. Five years later a design revision [2] was triggered by the evolving design parameters for  $\nu$ -facilities, the possibility of using the SPL as a EURISOL [3, 4] driver and the progress in the performance of SC bulk niobium cavities. The new design is devised to have maximum flexibility for the adaption to the needs of various (still evolving) neutrino schemes [5]. Without any hardware changes in the linac itself, the SPL can provide suitable beams for the  $\beta$ -beam/superbeam scenario and (possibly in a 2<sup>nd</sup> stage) to a full-blown  $\nu$ -factory [6]. It therefore allows a staged approach to  $\nu$ -physics which cannot be realised easily with other types of proton drivers such as rapid cycling synchrotrons. Furthermore the SPL beam can be time-shared with other high-power users (e.g. EURISOL), reducing the initial investment per user considerably.

The construction of the SPL is foreseen in three stages: i) currently approved and under construction: a 3 MeV test stand to characterise the performance and beam quality of the H<sup>-</sup> front-end including the beam chopper. This section is crucial for low-loss injection of the high-power beam into subsequent circular machines; ii) awaiting approval end 2006: construction of Linac4 [7], the normal conducting (NC) part of the SPL up to 160 MeV. Operating at low duty cycle, it will replace the existing proton Linac2 (50 MeV) and inject into the PSB; iii) relocation of Linac4, extension of the NC section to 180 MeV and the addition of a SC linac to reach an energy of 3.5 GeV. The approval for the last stage will depend on the European post-LHC physics road map (LHC upgrades, neutrino physics, linear collider, ...) and is not expected before 2010.

### SPL HIGH-POWER USERS

The present design foresees two modes of high-power operation: i)  $\nu$ -operation: 4 MW chopped H<sup>-</sup> pulses of 0.57 ms are accumulated in a subsequent ring via charge-exchange injection. The injection losses are minimised by cutting gaps into the bunch train corresponding to the transition time between RF (ring) buckets. In the reference scheme three out of eight bunches are removed by the low-energy beam chopper. ii) EURISOL operation: a 5 MW unchopped beam is sent directly onto a high-power target and one (or more) 100 kW beams are sent to low-power targets. Sending beam to different users within the same pulse can be done by either using the chopper to create 0.1 ms gaps in the bunch train allowing for the rise time of a switching magnet, or by using magnetic and/or laser stripping to remove a fraction of the beam for a low-power target. The 2<sup>nd</sup> option is under study by EURISOL and – given its success – would be preferable, since one can create longer pulses and thus reduce thermal stress in the target.

The energy of 3.5 GeV is an optimum for a beta-beam based neutrino facility on the CERN site, which is also reasonably compatible with the needs of EURISOL [8]. While the repetition rate of 50 Hz is well suited for neutrinos, it is also considered high enough for a EURISOL proton driver, even though a CW machine is the preferred driver in a "green field" scenario. Table 1 lists the main parameters of SPL I and of SPL II for  $\nu$  or EURISOL operation.

In parallel to the high-power users the SPL will provide

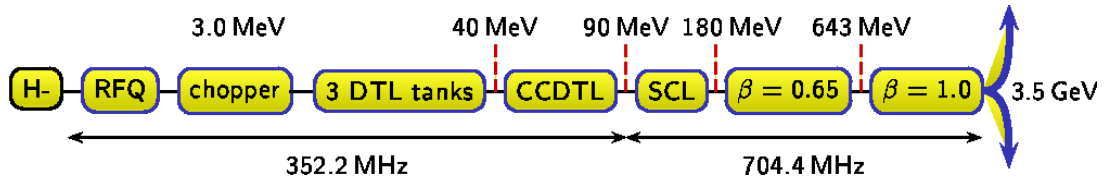


Figure 1: Schematic layout of the SPL.

a 1 Hz  $H^-$  beam to the CERN PS, replacing the PSB, and enabling a beam out of the PS that is compatible with all foreseen LHC luminosity upgrade scenarios.

## DESIGN AND IMPROVEMENTS TO SPL I

The layout of the SPL NC section ( $< 180$  MeV) is that of a classical high-power proton front-end: an RFQ [9] operating at 352.2 MHz accelerates the beam to 3 MeV. After the beam chopper a Drift Tube Linac (DTL) takes the beam to an energy of 40 MeV, followed by a Cell-Coupled DTL (CCDTL) up to 90 MeV. A Side Coupled Linac (SCL) at 704 MHz then accelerates the beam to 180 MeV (see also [7, 10]). Two families of SC five-cell bulk-niobium elliptical cavities then cover the energy range from 180 MeV to 3.5 GeV. The electric gradients of 19 and 25 MV/m, respectively, are based on electric and magnetic peak surface fields of  $E_{\text{peak}} = 50$  MV/m and  $B_{\text{peak}} = 100$  mT, values which are consistent with reported performances of bulk niobium structures [11, 12]. Figure 1 shows a block dia-

Table 1: Main linac parameters for SPL I and SPL II operating as driver for  $\nu$  production or EURISOL

	SPL I		SPL II	
	$\nu$	$\nu$	$\nu$	EURISOL
energy [GeV]	2.2	3.5	3.5	
length [m]	690	430	430	
av. beam power [MW]	4	4	5	
av. RF power <sup>†</sup> [MW]	24	17	21	
av. cryo power [MW]	9.6	3.6	4.4	
repetition rate [Hz]	75	50	50	
beam pulse length [ms]	2.2	0.57	0.71 + 0.014	
$I_{\text{av, pulse}}$ <sup>‡</sup> [mA]	11	40	40	
$I_{\text{peak}}$ <sup>‡</sup> [mA]	18.4	64	40	
beam duty cycle <sup>‡</sup> [%]	16.5	2.9	3.6	
chopping ratio [%]	75	62	–	
$\varepsilon_t$ , (r.m.s.) [ $\pi$ mm mrad]	0.4	0.36	0.36	
$\varepsilon_l$ , (r.m.s.) [ $\pi$ mm mrad]	0.76	0.5	0.5	
inj. turns (into ISR)	660	176	–	
peak RF power [MW]	32	162	162	
tetrodes*	79	3	3	
LEP klystrons**	44	14	14	
new klystrons***	–	44	44	
cryo temperature [K]	4.5	2	2	

without 30% margin for Lorentz detuning, <sup>‡</sup>  $> 3$  MeV,

\* 0.1 MW, 352 MHz, \*\* 1 MW, 352 MHz, \*\*\* 5 MW, 704 MHz

Table 2: Main parameters of the accelerating sections

Section	$E$ [MeV]	Cavit.	$\hat{P}_{\text{RF}}$ [MW]	Klystr.	$l$ [m]
Source	0.095	–	–	–	3
RFQ	3	1	1.0	1	6
Chopper	3	3	0.1	–	3.7
DTL	40	3	3.8	5	13.6
CCDTL	90	24	6.4	8	25.5
SCL	180	24	15.1	5	34.9
$\beta = 0.65$	643	42	18.5	7	86
$\beta = 1.0$	3560	136	116.7	32	256
<b>Total</b>	<b>3560</b>	<b>233</b>	<b>161.6</b>	<b>58</b>	<b>429</b>

gram of the SPL layout and Table 2 lists the main parameters of each accelerating section.

With respect to SPL I the power consumption was reduced by  $\approx 30\%$  for the RF system and by  $> 60\%$  for the cryogenic system. This is mainly due to i) the use of smaller SC cavities at 2 K (rather than 4.5 K), and ii) the raise in average pulse current. Both choices reduce the filling time of the cavities and thus reduce the ratio of RF pulse length over beam pulse length, resulting in a reduced RF duty cycle. The higher currents also increase the acceleration efficiency in the NC section by increasing the ratio of beam power over power dissipated in the copper structures. On the other hand more RF power at 704 MHz needs to be installed to cover the increased RF peak power.

The cryogenic system is based on the design of the TESLA/ILC cryo-modules [13, 14] taking into account the CERN LHC project experience [15]. All cryogenic piping as well as the SC quadrupoles are contained inside of the cryo-modules to reduce the amount of static losses and to minimise the overall length of the linac. Using long interconnected modules containing 6 to 8 high-gradient cavities each, it becomes possible to cover the energy range from 180 MeV to 3.5 GeV in less than 350 m.

For neutrino operation the SPL has to be complemented with circular machines to modify the pulse and bunch time structure: for the superbeam scenario an accumulator ring has to be added and for a  $\nu$ -factory an additional compressor ring is needed. First the linac burst is shortened to a length given by the circumference of the accumulator ( $\approx \mu\text{s}$ ) and then a compressor ring can be used to reduce the length of the single bunches to the ns range. Due to the increased bunch current and higher energy of SPL II, the linac pulse length was reduced from 2.2 ms to 0.57 ms. The shorter pulses have the double benefit of decreasing the number of injection turns into any subsequent circular

machine of a given size (e.g. the CERN PS) and of reducing the size of accumulator and/or compressor rings. Furthermore, the injection at higher energy reduces the space charge tune shift in the rings and allows for greater flexibility in the bunch structure that can be created with such an accelerator chain (compare [6]).

### BEAM DYNAMICS

Tracking studies have influenced the structural layout of the SPL from the first conception stage onwards. The main guidelines were the minimisation of r.m.s. emittance ( $\epsilon$ ) growth, halo development and losses by: i) keeping all zero-current tunes below  $90^\circ$ , ii) smoothing the tunes per metre across all transitions, and iii) avoiding  $\epsilon$ -exchange by keeping the longitudinal to transverse full-current tune ratio between 0.5 and 0.8 (adequate for the SPL emittance ratio of  $\epsilon_l/\epsilon_t \approx 1.4$ ). However, the concept of smooth transitions cannot be maintained in the chopper line, where a drastic change in the length of the focusing periods is unavoidable in order to house the deflecting plates. As a consequence the largest “local”  $\epsilon$ -growth occurs in the chopper line. It is limited to  $\approx 20\%$  by scraping the beam with a conical collimator which also acts as a beam dump for the chopped beam [16].

End-to-end simulations have been carried out starting from the RFQ input (95 keV) using a matched distribution with an r.m.s. relative energy spread of 0.5%, a value that we expect from the source extraction voltage jitter. The transverse  $\epsilon$  for the 70 mA input beam is  $0.25 \pi$  mm mrad and multi-particle simulations have been performed using uniform and Gaussian distributions. The beam performance is expected to be bound between these two cases which are reported in Table 3.

A large number of error runs has been used to establish the effects of statistical errors (quadrupoles: misalignment, displacement, rotation, gradient; RF fields: phase, amplitude) and to impose limitations on the machine tolerances (see [2, 17]). Using a Gaussian distribution the combined effect of all errors is expected to yield an additional 40-50%  $\epsilon$ -growth in the transverse plane and  $\approx 35\%$  in the longitudinal plane. For this simulation no losses are observed apart from the beam scraping in the chopper line.

Table 3: R.m.s. emittance growth in end-to-end simulations with uniform and Gaussian input distributions

	uniform in [%]			Gaussian in [%]		
	$\Delta\epsilon_x$	$\Delta\epsilon_y$	$\Delta\epsilon_z$	$\Delta\epsilon_x$	$\Delta\epsilon_y$	$\Delta\epsilon_z$
RFQ	9.3	8.4	–	8.5	10.6	–
Chopper	19.5	5.8	14.7	29.7	1.1	9.9
DTL	3	11	8.2	-2.4	20.7	11.9
CCDTL	-0.4	2	0.5	0.7	1.5	0.3
SCL	1.5	7.7	1.3	0.8	8.8	0.9
SC	0.3	0.4	4	0.3	0.4	4
total	36	39.7	26.4	40	49	25

### UPGRADE OPTIONS

In case of changing requirement for  $\nu$ -production or in case of additional users the SPL II is designed to offer ample scope for upgrades. The klystrons and accelerating structures are designed for a maximum duty cycle of 10% while the present design only uses half of this capability. Extending the beam pulse length but keeping a realistic safety margin a power upgrade to 8 MW seems feasible without major investment and is only limited by the availability of a suitable  $H^-$  source. Another upgrade option is an increase in beam energy which can be achieved by simply adding more SC modules. For each  $\approx 75$  m of additional SC modules the beam energy can be raised by 1 GeV. This upgrade path is somewhat limited by the increased difficulty to avoid  $H^-$  stripping via bending magnets and blackbody radiation in the transfer lines (see [2, 6, 18]). However, a factor of two gain in energy still seems feasible.

### REFERENCES

- [1] M. Vretenar (Ed.), Conceptual design of the SPL, CERN-2000-012.
- [2] F. Gerigk (Ed.), Conceptual design of the SPL II, CERN-2006-006.
- [3] EURISOL Design Study, <http://eurisol.org>
- [4] E. Noah *et al.*, EURISOL target stations operation and implications for its proton driver beam, CERN-AB-2006-055, EPAC06, Edinburgh.
- [5] BENE Steering Group, Beams for European neutrino experiments (BEBE), CERN-2006-005.
- [6] F. Gerigk, R. Garoby, Operational flexibility of the SPL as proton driver for neutrino and other applications, CERN-AB-2006-020, ICFA HB 2006, Tsukuba.
- [7] R. Garoby *et al.*, Linac4, a new injector for the CERN PS booster, CERN-AB-2006-027, EPAC06, Edinburgh.
- [8] J.E. Campagne and A. Caze, The  $\theta_{13}$  and  $\delta_{CP}$  sensitivities of the SPL-Fréjus project revisited, LAL-2004-102 (2004).
- [9] P.Y. Beauvais, Installation of the French high-intensity injector at Saclay, LINAC06, Knoxville.
- [10] M. Vretenar *et al.*, Design and development of RF structures for Linac4, LINAC06, Knoxville.
- [11] L. Lilje, High gradients in multi-cell cavities, 11th Workshop on RF Superconductivity, Travemünde 2003.
- [12] P. Pierini, Analysis of gradients for future high-current proton accelerators, ICFA HPSL 2005, Naperville.
- [13] TESLA Technical Design Report (2001): [http://tesla.desy.de/new\\_pages/TDR\\_CD/start.html](http://tesla.desy.de/new_pages/TDR_CD/start.html)
- [14] <http://www.interactions.org/linearcollider/gde>
- [15] LHC Design Report Volume 1, CERN-2004-003-V-1.
- [16] A.M. Lombardi *et al.*, End-to-end beam dynamics for CERN Linac4, ICFA HB 2006, Tsukuba.
- [17] M. Baylac *et al.*, Statistical simulations of machine errors for Linac4, ICFA HB 2006, Tsukuba.
- [18] W. Chou *et al.* 8 GeV  $H^-$  ions: transport and injection, PAC 2005, Knoxville.